

# Synthesis and Type I/Type II photosensitizing properties of a novel amphiphilic zinc phthalocyanine

Shaohua Wei<sup>a,b</sup>, Jiahong Zhou<sup>b</sup>, Deyin Huang<sup>a,\*</sup>, Xuesong Wang<sup>\*,c</sup>,  
Baowen Zhang<sup>c</sup>, Jian Shen<sup>b</sup>

<sup>a</sup> School of Chemistry and Chemical Technology, Shanghai JiaoTong University, Shanghai 200240, PR China

<sup>b</sup> Jiangsu Engineering Research Center for Bio-medical Function Material, Nanjing Normal University, Nanjing 210097, PR China

<sup>c</sup> Technical Institute of Physics and Chemistry, Chinese Academy of Sciences, Beijing 100101, PR China

Received 11 March 2005; received in revised form 29 April 2005; accepted 15 June 2005

Available online 28 September 2005

## Abstract

A novel amphiphilic zinc phthalocyanine (ZnPcLTs) has been synthesized, which possesses good amphiphilicity, and low aggregation. The generation efficiency of singlet oxygen and other active oxygen species' trapping rate studies were studied by electron spin resonance (ESR) spectroscopy. The results indicated that the photosensitizer possessed a higher active oxygen species generation efficiency than that of hematoporphyrin. The results of photodamage experiments towards calf-thymus DNA indicated that ZnPcLTs is a promising photosensitizer candidate for photodynamic therapy.

© 2005 Elsevier Ltd. All rights reserved.

**Keywords:** Sulfonated zinc phthalocyanine; Active oxygen; Amphiphilicity; ESR; PDT

## 1. Introduction

Sulfonated zinc and aluminum phthalocyanine derivatives have attracted a considerable amount of attention as second-generation photosensitizers for treatment of malignant tumors by photodynamic therapy (PDT) in the last decade [1–3]. Their PDT efficiency not only depends on the formation of the cytotoxic species ( $^1\text{O}_2$ ,  $\text{O}_2^{\cdot-}$  and  $\text{OH}^{\cdot}$ ) but also depends on the amphiphilicity of photosensitizer [4,5]. Since a hydrophilic character benefits the transport of a drug in the body, and its lipophilicity benefits its uptake by tumor cells, the amphiphilicity of a photosensitizer is therefore considered to be an important factor in the design of a new photosensitizer [6–8]. Phthalocyanines have been studied as potential PDT photosensitizers;

but, the large conjugated  $\pi$ -system leads to a strong stacking tendency in solution, which usually decreases their luminescence quantum yield, shortens their triplet state lifetime by enhancement of internal conversion, and so reduces their photosensitizing efficiency. The dye is more active in its monomeric state [9,10]. It is, therefore, important to develop a phthalocyanine which is both amphiphilic and nonaggregated, but the study of these compounds for use in PDT is still in its infancy [2,11,12].

Of the phthalocyanines, zinc phthalocyanine tetrasulfonate (ZnPcTs) has been more investigated as a PDT photosensitizer. Since it is not only highly aggregated in aqueous solution, as shown by spectroscopic studies, but is also a strongly hydrophilic photosensitizer, its photodynamic activity is lower than its disulfonate analogue (ZnPcDs), which has more amphiphilic structure [2,6,13]. We report herein the synthesis and photophysical properties of a novel zinc phthalocyanine (ZnPcLTs) containing sulfonated naphthoxy substituents (shown in

\* Corresponding authors. Tel./fax: +86 21 547 47445.

E-mail address: [dyhuang@sjtu.edu.cn](mailto:dyhuang@sjtu.edu.cn) (D. Huang).

Fig. 1). The introduction of naphthoxy substituents not only enhances the lipophilic character of the molecule, but also prevents its molecular aggregation in solution for steric reason, potentially resulting in superior photophysical characteristic enhanced PDT properties.

## 2. Experimental

### 2.1. Materials

2,2,6,6-Tetraethyl-4-piperidone (TEMP), 5,5-dimethyl-1-pyrroline-*N*-oxide (DMPO), 1,4-diazabicyclo[2,2,2]octane (DABCO), superoxide dismutase (SOD), sodium benzoate and 9,10-diphenylanthracene (9,10-DPA) were all purchased from Aldrich Chemical Company, USA. Dimethylsulfoxide (DMSO), hematoporphyrin and other reagents of analytical grade were obtained from Beijing Chemical Plant. 4-Nitrophthalonitrile was prepared and purified according to the methods described in the literature [14]. All reaction solvents were dried over molecular sieve of 4 Å and further distilled before use.

### 2.2. Equipments

IR spectra were recorded on a PARAGN1000 FT-IR spectrometer using KBr pellets. The absorption and the fluorescence spectra were measured with LAMBDA20/2.0 spectrometer and Hitachi F-4500 fluorescence spectrophotometer, respectively.  $^1\text{H}$  NMR spectra were

obtained in  $\text{D}_2\text{O}$  on a Gemini-2000 analyzer (300 MHz, Varian Ltd.).

### 2.3. Synthesis of 4-(5-sulfo-1-naphthoxy)-phthalonitrile

4-Nitrophthalonitrile (3.46 g, 0.02 mol) and 5-hydroxy-1-naphthalene sulfonic acid (6.72 g, 0.03 mol) were dissolved in 50 ml of dry DMSO at room temperature. The mixture was stirred, and 5.52 g (0.04 mol) of anhydrous potassium carbonate was added over a period of 1 h under a nitrogen atmosphere. The same amount of potassium carbonate was then added after 8 h of stirring at room temperature. After about 20 h the mixture was poured into 250 ml of 1 M hydrochloric acid. After settling of the suspension within 8 h, the crude product was collected by vacuum filtration and washed with ethanol. The isolated product (yellow needles 3.85 g, 55%) was recrystallized from methanol. IR ( $\text{cm}^{-1}$ ): 3440, 3100–3000 (Ar, H), 2233 (Ar–C $\equiv$ N), 1598, 1570, 1493 (Ar), 1277, 1250 (Ar–O–Ar), 1200 (S–O), 785, 656 (C–S).  $^1\text{H}$  NMR ( $\text{D}_2\text{O}$ ):  $\delta$  8.46–7.98 (m, 3H, H–Ar(CN) $_2$ ),  $\delta$  7.75–7.34 (m, 6H, H–ArSO $_3\text{H}$ ). Elemental analysis: ( $\text{C}_{18}\text{H}_{10}\text{N}_2\text{O}_4\text{S}$ , FW 350). Calc: C, 61.71; H, 2.88; N, 8.00; found: C, 61.46; H, 2.84; N, 7.92.

### 2.4. Preparation of ZnPcLTs

4-(5-Sulfo-1-naphthoxy)phthalonitrile (1.05 g, 3 mmol), 1-pentanol (25 ml) and DBU (1.5 ml) were mixed. The mixture was stirred at 70 °C for 10 min in a nitrogen atmosphere, then 0.1 g (0.8 mmol) of anhydrous zinc

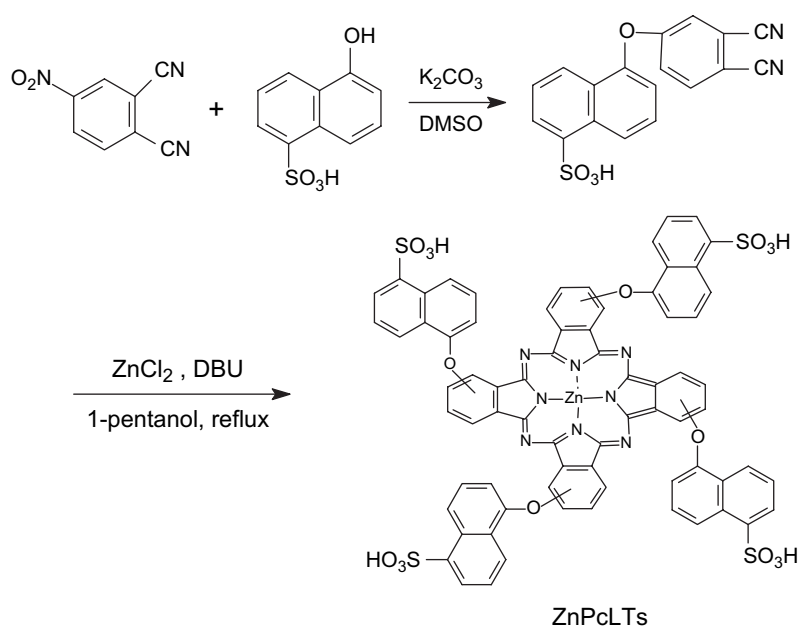
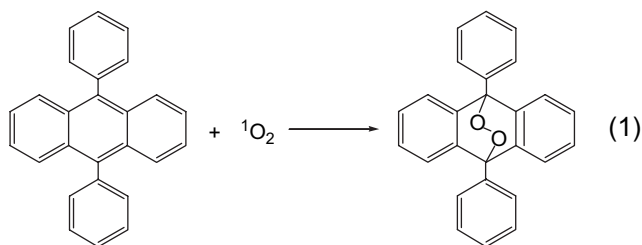


Fig. 1. The chemical structure of the phthalocyanine ZnPcLTs.

chloride was added. The suspension was slowly brought to boiling over a period of 1 h and refluxed for 36 h. The reaction mixture was cooled to 60 °C, and 50 ml of methanol was added. The deep blue product was filtered off, washed with hydrochloric acid (0.1 mol/l, 2 × 100 ml) and then with acetone (2 × 50 ml). The crude product was extracted with dichloroethane and acetone in a Soxhlet extractor, and purified by column chromatography (silica gel, THF–toluene, 8:2). The blue fraction was collected, evaporated under vacuum and dried in vacuo at 100 °C. Yield: 0.57 g (51.8%), deep blue powder. IR (cm<sup>-1</sup>): 3441, 3000–2800 (Ar, H), 1650, 1418, 1348, 1247 (Ar–O–Ar), 1214 (S–O), 785, 664 (C–S). NMR (CDCl<sub>3</sub>): δ 7.2–7.55 (m, 28, Ar–H). Elemental analysis: (C<sub>72</sub>H<sub>40</sub>N<sub>8</sub>O<sub>16</sub>S<sub>4</sub>Zn, FW 1465). Calc: C, 58.96; H, 2.75; N, 7.64; found: C, 58.72; H, 2.84; N, 7.51.

### 2.5. Quantum yield of <sup>1</sup>O<sub>2</sub> generation

The quantum yields of <sup>1</sup>O<sub>2</sub> generation for ZnPcLTs were determined using the 9,10-DPA bleaching method (taking hematoporphyrin as a reference) [15]. The photo-oxidation of DPA sensitized by ZnPcLTs was carried out in a ‘merry-go-round’ apparatus, using a high-pressure mercury lamp (500 W) as the light source in combination with a 578-nm monochromatic filter. During the measurements, the optical densities at 436 nm of the samples examined were adjusted to be the same. The reactions were followed spectrophotometrically by observing the decrease in the 374 nm absorption peak of 9,10-DPA as a function of irradiation time.



### 2.6. EPR experiments

EPR spectra were obtained using a Bruker ESP-300E spectrometer operating at room temperature, and the operating conditions were as follows: microwave bridge: X-band with 100 Hz field modulation; sweep width: 100 G; modulation amplitude: 1.0 G; modulation frequency, 100 kHz; receiver gain: 1 × 10<sup>5</sup>; microwave power: 5 mW. Samples were injected into the specially made quartz capillaries for EPR analyses, and purged with argon or air for 30 min in the dark, respectively, according to the experimental requirement and illuminated directly in cavity of the ESR spectrometer with a Nd:YAG laser (532 nm, 5–6 ns of pulse

width, repetition frequency: 10 Hz, 10 mJ/pulse energy). The kinetics of spin adduct generation were studied by recording peak heights of EPR spectra every 30 s. To make the production efficiencies of all spin adducts comparable, concentrations of ZnPcLTs and hematoporphyrin were adjusted to keep the same optical density at 532 nm.

### 2.7. Ethidium bromide (EB) assay for CT DNA cleavage

A simple assay for DNA cleavage was applied based on ca. 20-fold enhancement of the fluorescence intensity exhibited by EB upon intercalation into DNA [16,17]. When the concentration of EB is more than two folds than that of DNA base pair, fluorescence intensity of EB is linearly proportional to the concentration of DNA base pair. Any process in which the potential EB binding site was destroyed results in a decrease in fluorescence intensity.

After preparation of solutions of EB/DNA buffer solution (0.1 mM Triton, 80 μM EB, 40 μM CT DNA), ZnPcLTs or hematoporphyrin was added into 10 ml of EB/DNA buffer solution, and the final concentration of ZnPcLTs or hematoporphyrin was 10 μM. These mixture solutions were divided into 5 aliquots and irradiated in a ‘merry go round’ apparatus with a medium pressure sodium lamp (hν > 470 nm). The aliquots were removed at various time and analyzed with fluorescence emission spectrum measured from 525 to 800 nm and excited at 510 nm.

The percentage of binding site remaining at a given time (*t*) was calculated from the following Eq. (2):

$$\text{Binding site remaining (\%)} = 100 \times \left( 1 - \frac{I_0 - I_t}{I_0 - I_{\text{buf}}} \right) \quad (2)$$

where *I*<sub>0</sub>, *I*<sub>*t*</sub>, *I*<sub>buf</sub> denote the integrated fluorescence intensities before irradiation, after *t* min of irradiation, and of DNA-free buffer, respectively.

## 3. Results and discussion

### 3.1. Synthesis and characterization of ZnPcLTs

4-(5-Sulfo-1-naphthoxy)phthalonitrile was prepared in moderate yield from 4-nitrophthalonitrile by the method described in the literature [14,18]. ZnPcLTs was prepared from this phthalonitrile derivative and anhydrous zinc(II) chloride, catalyzed by DBU in anhydrous 1-pentanol. The reaction conditions were mild and the yield of product was 51.8%. This procedure yielded a mixture of four regioisomers with a 5-sulfonaphthoxy group at the 2- or 3-positions of each benzene ring in the ZnPcLTs molecule [10]. Elemental analysis and

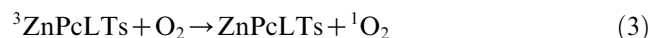
spectroscopic data (IR,  $^1\text{H}$  NMR and UV–vis) confirmed the assigned structure for ZnPcLTs.

As the introduction of naphthoxy substituents enhances the lipophilic character, and the sulfonic acid substituents give hydrophilic character to the compound, thus ZnPcLTs possesses amphiphilic character. It was highly soluble in ethanol and DMSO, moderately soluble in water, pyridine and propyl alcohol and less soluble in chloroform. Due to the steric hindrance of the peripheral naphthoxy substituents, these enlarge the approachable distance between two neighbouring macrocycles, which could help to lower the tendency to form stacked aggregates. The UV–vis absorption spectra of ZnPcLTs in different solvents are shown in Fig. 2. There are usually two long wavelength peaks for phthalocyanine derivatives [9,19]; one (635 nm) corresponds to aggregate absorption, while the other (677 nm) is due to absorption by the monomeric molecule. The ZnPcLTs absorption spectrum in water shows only the aggregate absorption at 634 nm, whereas in the case of ZnPcLTs the monomer band at 677 nm is enhanced and the aggregate absorption at 635 nm becomes lower. When ethanol (or DMSO) is employed as a solvent, the ZnPcLTs absorption spectrum shows only the monomer band at 678 nm. This phenomenon indicates that aggregated ZnPcLTs is not significant in ethanol (or DMSO), and shows a lower tendency to form aggregates than ZnPcTs in water.

### 3.2. Singlet oxygen generation

It has previously been reported that a nitroxide radical was detectable by EPR when 2,2,6,6-tetraethyl-4-piperidone-*N*-oxy-radical (TEMPO) was generated from the reaction of TEMP with singlet oxygen ( $^1\text{O}_2$ ) [20]. When the air-saturated DMSO solution of ZnPcLTs (10  $\mu\text{M}$ ) was irradiated for 1 min, and TEMP

(10 mM) was used as a spin trap, an ESR spectrum of triplet peaks with equal intensity, characteristic of a nitroxide radical, was observed (Fig. 3, spectrum a). The hyperfine splitting constant of the photosensitized oxidation product of TEMP by ZnPcLTs was 16.0 G, which was identical with the simulated spectrum of a nitroxide radical (Fig. 3, spectrum b) and those of TEMPO in the literature [21]. Under similar conditions but in the absence of ZnPcLTs or oxygen or irradiation, TEMPO formation did not occur (Fig. 3, spectrum c). To provide further evidence to support the involvement of  $^1\text{O}_2$  in this photosensitizing process, DABCO, a specific  $^1\text{O}_2$  scavenger, was added into the solution of ZnPcLTs. After irradiation for 1 min, the ESR signal of TEMPO was also observed, but the intensity was suppressed (Fig. 3, spectrum d). These phenomena suggest that TEMPO is derived from the reaction of TEMP with  $^1\text{O}_2$  generated via the energy transfer from excited triplet ZnPcLTs to ground state oxygen by the irradiation of ZnPcLTs (Eq. (3)).



According to previous papers, the  $^1\text{O}_2$  plays an important role in the PDT process, and consequently the quantum yield of  $^1\text{O}_2$  is a useful parameter for determining the phototherapeutic activity of the photodynamic agent. The photo-oxidation of 9,10-DPA to its endoperoxide derivative by singlet oxygen has often been used to detect  $^1\text{O}_2$  and to determine the quantum yield of  $^1\text{O}_2$  formed by photosensitization (9,10-DPA bleaching method). In order to determine the quantum

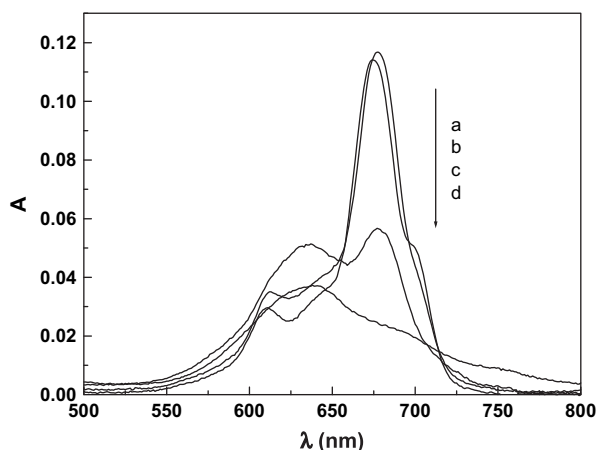


Fig. 2. Absorption spectra of a: ZnPcLTs in ethanol; b: ZnPcLTs in propyl alcohol; c: ZnPcLTs in water; d: ZnPcTs in water. Concentration:  $1.21 \times 10^{-6}$  M.

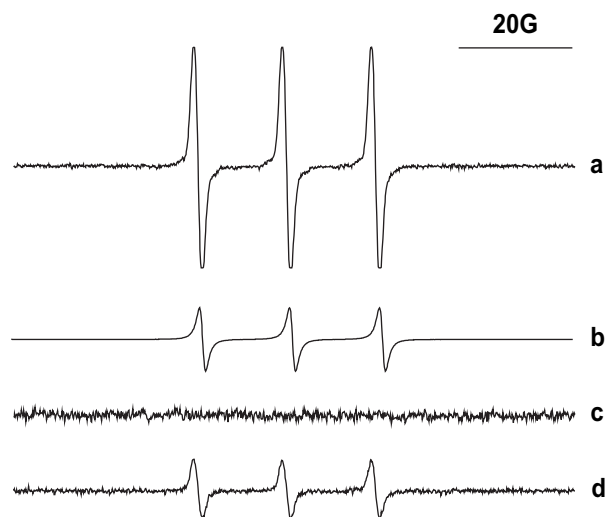


Fig. 3. Spectrum a: photoinduced EPR spectrum from an air-saturated DMSO solution of ZnPcLTs (10  $\mu\text{M}$ ) and TEMP (10  $\mu\text{M}$ ) on illumination for 1 min; spectrum b: the simulated spectrum of nitroxide radical; spectrum c: same as spectrum (a) but in the absence of ZnPcLTs, oxygen or light; spectrum d: same as spectrum (a) but in the presence of DABCO (20  $\mu\text{M}$ ).

yield of  $^1\text{O}_2$  generation by ZnPcLTs, the 9,10-DPA bleaching method was adopted (using hematoporphyrin as a reference). Fig. 4 shows the bleaching of 9,10-DPA photosensitized by ZnPcLTs. Fig. 5 shows the bleaching of 9,10-DPA both by ZnPcLTs and hematoporphyrin as a function of irradiation time at 436 nm in DMSO solution. Control experiments indicated that no 9,10-DPA bleaching occurred when ZnPcLTs or hematoporphyrin, oxygen or irradiation was omitted. From Fig. 5, the  $^1\text{O}_2$  generation quantum yield of ZnPcLTs was calculated to be 1.26, assuming that the  $^1\text{O}_2$  generation quantum yield of hematoporphyrin was unity.

### 3.3. Superoxide anion radical generation

DMPO spin trapping has been successfully applied to detect certain reactive intermediates, such as  $\text{O}_2^{\cdot-}$  and hydroxyl radical, because it has a high affinity for these reactive radicals and leads to the formation of persistent spin adducts. When an air-saturated DMSO solution of ZnPcLTs and DMPO was irradiated with 532 nm light, a new EPR spectrum appeared (Fig. 6). This EPR spectrum could be characterized by three hyperfine coupling constants:  $\alpha^{\text{N}} = 13.0$  G,  $\alpha_{\beta}^{\text{H}} = 10.1$  G, and  $\alpha_{\gamma}^{\text{H}} = 1.5$  G [22], due to the nitrogen and two hydrogen atoms at the  $\beta$  and  $\gamma$  positions, and was consistent with previously reported values for the  $\text{DMPO-O}_2^{\cdot-}$  adduct. Compared with hematoporphyrin, the  $\text{DMPO-O}_2^{\cdot-}$  signal intensity of ZnPcLTs was higher. Again, this signal could not be detected in the dark, or upon irradiation but omitting any of the sample components.

The kinetics of  $\text{DMPO-O}_2^{\cdot-}$  signal generation was also studied by irradiating ZnPcLTs or hematoporphyrin (Fig. 7), the results show that the quantum yield of

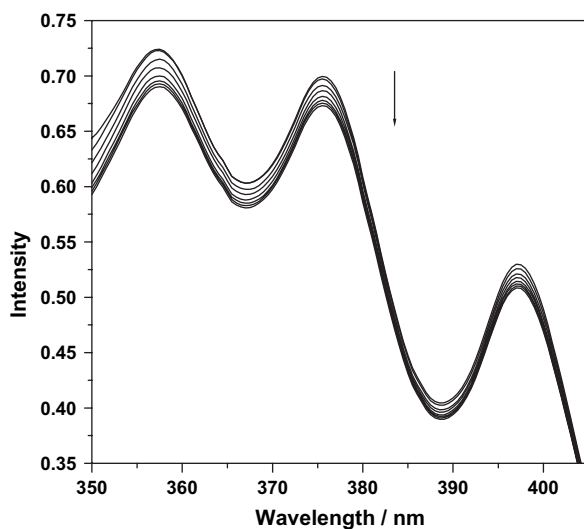


Fig. 4. The absorption spectra in the DPA bleaching system upon irradiation ZnPcLTs. The arrow indicates the direction of change.

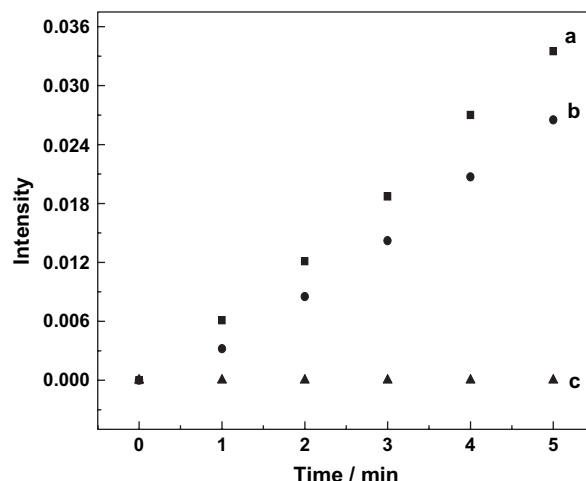


Fig. 5. The results of the photosensitized DPA bleaching by irradiating ZnPcLTs and DPA (line a); line b: same as line a except that ZnPcLTs was replaced by hematoporphyrin; line c: control experiment.

$\text{O}_2^{\cdot-}$  of ZnPcLTs was about 1.5 times than that of hematoporphyrin by the ESR signal intensity of  $\text{DMPO-O}_2^{\cdot-}$ .

### 3.4. $\text{OH}^{\cdot}$ generation

If water was present in an air-saturated DMSO solution of ZnPcLTs and DMPO, irradiation with the laser at 532 nm gave an ESR spectrum of the spin adduct  $\text{DMPO-OH}^{\cdot}$  (Fig. 8, spectrum a), which was characterized by two coupling constants connected with the non-zero nuclear spins of nitrogen atom and hydrogen atom in the  $\beta$  position:  $\alpha^{\text{N}} = \alpha^{\text{H}} = 14.9$  G. The two identical coupling constants from  $\beta$ -N and  $\beta$ -H

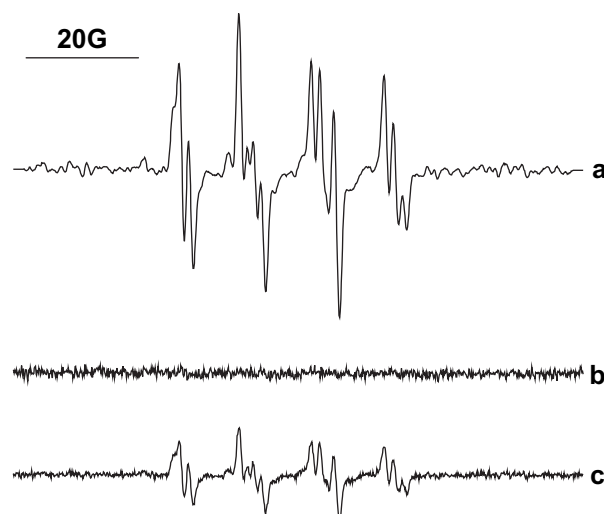


Fig. 6. Spectrum a: photoinduced EPR spectrum from an air-saturated DMSO solution of ZnPcLTs (10  $\mu\text{M}$ ) and DMPO (10  $\mu\text{M}$ ) on illumination for 1 min; spectrum b: same as spectrum (a) but in the absence of ZnPcLTs, oxygen or light; spectrum c: same as spectrum (a) but in the presence of SOD (20  $\mu\text{M}$ ).



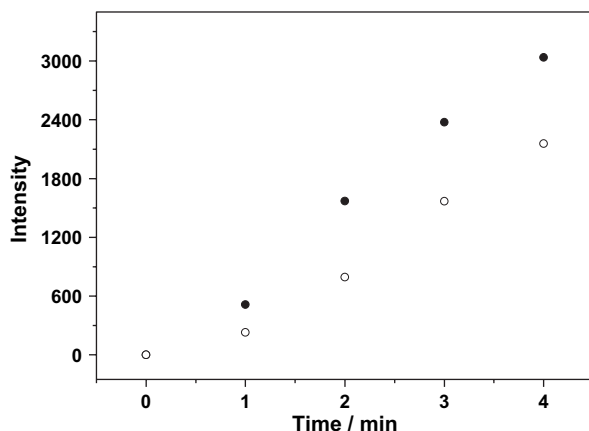


Fig. 7. Dependence of the DMPO–superoxide radical adduct intensity on irradiation time derived from irradiation of an air-saturated DMSO solution containing ZnPcLTs (10  $\mu$ M) (●) or hematoporphyrin (10  $\mu$ M) (○) and DMPO (10  $\mu$ M).

gave a four-line ESR spectrum with a density ratio of 1:2:2:1. These coupling constant values were in good agreement with the literature [23]. In aqueous solution  $O_2^-$  underwent rapid dismutation to form  $H_2O_2$  and which then further transformed to  $OH^\cdot$ . In the presence of sodium benzoate, a scavenger of hydroxyl radical, the ESR signal was decreased significantly (Fig. 8, spectrum b). Control experiments ensured that no signal was obtained without light, oxygen, ZnPcLTs, or DMPO (Fig. 8, spectrum c). These observations confirmed the assignment of the signal in the spectrum a to the DMPO– $OH^\cdot$  radical adduct.

The generation of  $O_2^-$ ,  $OH^\cdot$  and  $^1O_2$  by ZnPcLTs photosensitization indicated that ZnPcLTs maintained a photodynamic activity in terms of Type I and Type II

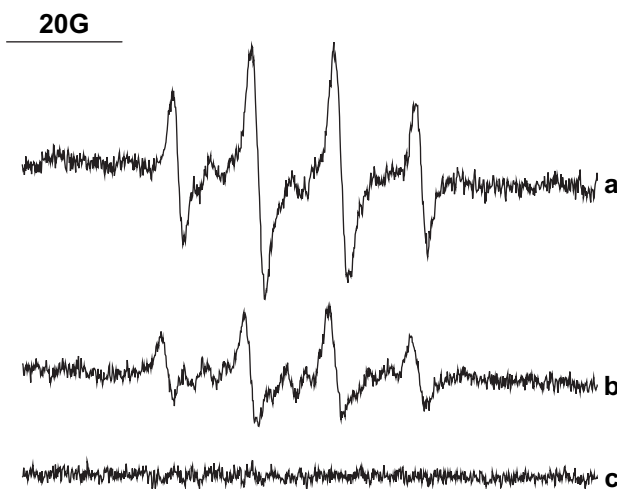


Fig. 8. Spectrum a: ESR spectrum of DMPO–hydroxyl radical adduct resulted from irradiation of an air-saturated buffer solution of ZnPcLTs (10  $\mu$ M) and DMPO (10  $\mu$ M). Spectrum b: similar to spectrum a, but in the presence of sodium benzoate (10  $\mu$ M). Spectrum c: removal of ZnPcLTs, oxygen or light.

mechanisms. All the above results suggest that ZnPcLTs is a promising candidate as a PDT sensitizer.

### 3.5. Photoinduced damage to CT DNA

Although it has been shown that ZnPcLTs possesses potential photodynamic activity in terms of Type I and Type II mechanisms, its ability to induce biological photodamage needed to be tested. This was examined by measuring its ability to cause photoinduced damage to CT DNA.

To study the PDT properties of ZnPcLTs, CT DNA in air-saturated buffer solution (10 mM acetic acid ammonium salt, 100 mM sodium chloride, pH = 7.0) was used as a phototherapeutic target and the ethidium bromide (EB) assay was adopted to follow the photodamage. The results are shown in Fig. 9. Using Eq. (2), 33.70% binding sites were calculated to be destroyed during a 50-min irradiation with light above 463 nm in EB–CT DNA buffer solution containing 10  $\mu$ M of ZnPcLTs, while only 20.91% binding sites were damaged with the same concentration of hematoporphyrin as sensitizer under aerobic conditions.

## 4. Conclusion

In summary, the demonstrated properties of good amphiphilicity and low aggregation suggest that ZnPcLTs should be absorbed by tumor cells easily. In addition, ZnPcLTs exhibited a high active oxygen species generation efficiency, which indicates that it could photodamage tumor tissue in terms of Type I and Type II mechanisms. Furthermore, the results of CT DNA photodamage experiments suggested that the photodamage ability of ZnPcLTs was higher than that of hematoporphyrin. Thus ZnPcLTs has its promising potential as PDT photosensitizer.

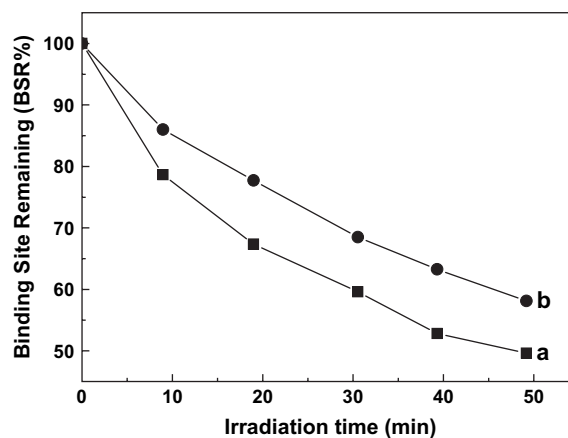


Fig. 9. The photodamage abilities of ZnPcLTs (line a) and hematoporphyrin (line b) with the irradiation time.

## Acknowledgements

The authors thank Natural Science Foundation of Jiangsu Education Department (Grant NO. 03KJB150059 and 04KJB150068) for the support.

## References

- [1] Foley MSC, Beeby A, Parker AW, Bishop SM, Phillips D. Photophysics of disulphonated aluminium phthalocyanine in reverse micelles of aerosol OT. *J Photochem Photobiol B* 1997;38:18–24.
- [2] Owens JW, Robins M. Phthalocyanine photophysics and photosensitizer efficiency on human embryonic lung fibroblasts. *J Porphyrins Phthalocyanines* 2001;5:460–4.
- [3] Vrouenraets MB, Visser GWM, Stigter M, Oppelaar H, Snow GB, Vandongen AMS. Comparison of aluminum(III) phthalocyanine tetrasulfonate and *meta*-tetrahydroxyphenyl-chlorin-monoclonal antibody conjugates for their efficacy in photodynamic therapy in vitro. *Int J Cancer* 2002;98:793–8.
- [4] Decreau R, Richard MJ, Julliard M. Photodynamic therapy against achromic M6 melanocytes: phototoxicity of lipophilic axially substituted aluminum phthalocyanines and hexadecahalogenated zinc phthalocyanines. *J Porphyrins Phthalocyanines* 2001;5:390–6.
- [5] Foley MSC, Beeby A, Parker AW, Bishop SM, Phillips D. Excited triplet state photophysics of the sulphonated aluminium phthalocyanines bound to human serum albumin. *J Photochem Photobiol B* 1997;38:10–7.
- [6] Huang JL, Chen NS, Huang JD, Liu ES, Xue JP, Yang SL, et al. Metal phthalocyanine as photosensitizer for photodynamic therapy (PDT)—preparation, characterization and anticancer activities of an amphiphilic phthalocyanine  $\text{ZnPcS}_2\text{P}_2$ . *Sci China Ser B* 2001;44:113–22.
- [7] András G, Péter B, István B, Viktor C, Mikós K, Klára S, et al. Triple state properties of tetrasubstituted zinc phthalocyanine derivatives. *J Mol Struct* 2004;704:11–5.
- [8] Sakamoto K, Kato T, Ohno-Okumura E, Watanabe M, Cook MJ. Synthesis of novel cationic amphiphilic phthalocyanine derivatives for generation photosensitizer using photodynamic therapy of cancer. *Dyes Pigments* 2005;64:63–71.
- [9] Drechsler U, Pfaff M, Hanack M. Synthesis of novel functionalised zinc phthalocyanines applicable in photodynamic therapy. *Eur J Org Chem* 1999;3441–53.
- [10] Fernández DA, Awruch J, Dixelio LE. Synthesis and photophysical properties of a new cationic water-soluble Zn phthalocyanine. *J Photochem Photobiol B* 1997;38:227–32.
- [11] Ng ACH, Li Xi-you, Ng DKP. Synthesis and photophysical properties of nonaggregated phthalocyanines bearing dendritic substituents. *Macromolecules* 1999;32:5292–8.
- [12] Fu J, Li XY, Ng Dennis KP, Wu C. Encapsulation of phthalocyanines in biodegradable poly(sebacic anhydride) nanoparticles. *Langmuir* 2002;18:3843–7.
- [13] Chatlani PT, Bedwell J, MacRobert AJ, Barr H, Boulos PB, Krasner N, et al. Comparison of distribution and photodynamic effects of di- and tetrasulfonated aluminum phthalocyanines in normal rat colon. *Photochem Photobiol* 1991;53:745–51.
- [14] Young JG, Onyebuagu W. Synthesis and characterization of di-disubstituted phthalocyanines. *J Org Chem* 1990;55:2155–60.
- [15] Diwu ZJ, Lown JW. Photosensitization with anticancer agents. 12. Perylenequinonoid pigments, a novel type of singlet oxygen sensitizer. *J Photochem Photobiol A Chem* 1992;64:273–87.
- [16] Pruetz WA. Inhibition of DNA—ethidium bromide intercalation due to free radical attack upon DNA. (I) Comparison of the effects of various radical. *Radiat Environ Biophys* 1984;23:1–6.
- [17] Pruetz WA. Inhibition of DNA—ethidium bromide intercalation due to free radical attack upon DNA. II. Copper(II)-catalysed DNA damage by  $\text{O}_2^-$ . *Radiat Environ Biophys* 1984;23:7–18.
- [18] Wei SH, Huang DY, Li L, Meng QH. Synthesis and properties of some novel soluble metallophthalocyanines containing 3-trifluoromethylphenoxy moiety. *Dyes Pigments* 2003;56:1–6.
- [19] Şaşmaz Selami, Ağar Erbil, Ağar Ayşen. Synthesis and characterization of phthalocyanines containing phenothiazine moieties. *Dyes Pigments* 1999;42:137–42.
- [20] Moan J, Wold E. Detection of singlet oxygen production by ESR. *Nature* 1979;279:450–1.
- [21] Lion Y, Delmelle M, Vorst AV. New method of detecting singlet oxygen production. *Nature* 1976;263:442–3.
- [22] Harbour JR, Hair ML. Detection of superoxide ions in non-aqueous media. Generation by photolysis of pigment dispersions. *J Phys Chem* 1978;82:1397–9.
- [23] Lang K, Wagnerova M, Stopka P, Dameran W. Reduction of dioxygen to superoxide photosensitized by anthraquinone-2-sulphonate. *J Photochem Photobiol A Chem* 1992;67:187–95.